STUDY OF HYDROXYAPATITE BY THERMOANALYTICAL METHODS

Lenka ŠIMKOVÁ, Petra ŠULCOVÁ

Department of Inorganic Technology, Faculty of Chemical Technology, University of Pardubice, Doubravice 41, 532 10 Pardubice, Czech Republic
e-mail: lenka.simkova1@student.upce.cz

INTRODUCTION

The title "apatite" refers to a group of compounds with a general formula in form $M_{10}(XO_4)_6Z_2$, where Z^- may be typically OH^-, F^-, Cl^- [1]. Hydroxyapatite (HAP) has the molecular structure of apatite, where M is calcium (Ca^{2+}), X is phosphorus (P^{5+}) and Z is the hydroxyl group (OH^-). This composition of elements is known as stoichiometric hydroxyapatite and its atomic ratio of Ca/P is 1.67. The chemical formula of HAP is $Ca_{10}(PO_4)_6(OH)_2$, with 39.89 % by weight of calcium, 18.50 % of phosphorus, 41.41 % of oxygen and 0.20 % of hydrogen [2, 3].

The reason for the enlargement of phosphate pigments is rigorous environmental and hygienic limits, which demand the replacement of toxic pigments (e.g. lead, chromate) with nontoxic but very effective pigments [4]. It is known, that HAP is a stable apatite compound and has been used widely due to its resemblance to human bone composition, bioactivity, and biocompatibility [5]. Consequently, HAP was considered as a bioactive material for synthetic bone replacement due to its chemical and biological affinity and biocompatibility with bone tissue [6].

The most common form of HAP is the hexagonal crystal structure, $P6_3/m$ space group, with Ca/P ratio 1.67 [7]. Stoichiometry, pH, temperature, and rate of reagent addition influence the precipitation of HAP. Therefore, it is crucial to control these aspects to produce HAP with an optimum morphology and crystallinity [8]. The optimum Ca/P molar ratio must be 1.667. However one of the main problems related to HAP processing is the low stability of HAP at temperatures near to the sintering range, which is attributed to deviations from the ideal Ca/P ratio [9]. In addition, a lot of factors contribute to complicating the image: sample structure, particle size, purity, powders surface condition, and particles aggregation can support undesirable decompositions and phase transitions [10]. In consequence, several compounds can be formed such as oxyapatite (OHA), oxyhydroxyapatite (OHAP), β–tricalcium phosphate (β–TCP), calcium oxide (CaO) and tetracalcium phosphate (T–TCP) [11, 12]. Particularly the formation of β–TCP ($Ca_3(PO_4)_2$) as the most likely phenomenon in the decomposition process highlights the importance of the Ca/P ratio in the control of HAP stability [10].

The aim of this work is the synthesis of hydroxyapatite powders by the precipitation method with different Ca/P ratios (1; 1.67; 3), pH (7; 12) and the same rate of precipitation (2 ml/min). The synthesized powders were characterized by X-ray diffraction in order to identify the phase composition and crystallinity (XRD); the elemental composition was investigated by X-ray photoelectron spectroscopy (XPS); the powders were analyzed for particle size distribution and the thermal behavior of powders was explored by thermal analysis DTA/TG.

EXPERIMENTAL PART

For a purpose to select convenient synthesis conditions for the formation of hydroxyapatite phase, the thermodynamic stability of the hydroxyapatite $Ca_{10}(PO_4)_6(OH)_2$

in aqueous solution was analyzed and approved in laboratory conditions [13]. It was found that hydroxyapatite is stable in the pH range from 4.8 to 14. Due to this information, three Ca/P ratios were chosen for the synthesis of hydroxyapatite, which was studied at pH = 7 and pH = 12. Ca/P = 1: in this case, HAP formation occurs in excess of phosphate ions; Ca/P = 1.67: this corresponds to the Ca/P stoichiometry of hydroxyapatite, which is 10/6; Ca/P = 3: HAP formation occurs in excess of calcium ions.

Altogether, 4 samples were synthesized at different synthesis conditions (Table 1, precipitation rate of 2 ml/min). The prepared powders were aged during 24 hours, filtered and washed with distilled water to neutral pH, then dried at 80 °C for 6 h. Characterization of the prepared powders was then performed by XRD, XPS and DTA/TG analysis.

Tab. 1 *Overview of the obtained samples and the synthesis conditions.*

Sample	Composition	Ca/P ratio	pH
1	$Ca_{10}(PO_4)_6(OH)_2$	1	7
2	$Ca_{10}(PO_4)_6(OH)_2$	1.67	7
3	$Ca_{10}(PO_4)_6(OH)_2$	3	7
4	$Ca_{10}(PO_4)_6(OH)_2$	1.67	12

The phase analysis of the powdered materials was studied by X-ray diffraction analysis (XRD). The phase composition was determined using diffractometer MiniFlex 600 (Rigaku, Japan) equipped with a vertical goniometer of 17 cm in the 2θ range of 10°–50°. The accuracy of goniometer was ±0.02°. X-ray tube with Cu anode (U = 40 kV, I = 15 mA) was used (CuKα radiation). The results were evaluated using the PDF-2 database. The elemental composition of the powders was studied by X-ray photoelectron spectroscopy (XPS) equipped ESCA 2SR (Scienta Omicron) with ultra – high vacuum apparatus. The thermal stability of samples was followed by simultaneous thermal analysis using the STA 449C Jupiter (NETZSCH, Germany) which allows simultaneous registration of the thermoanalytical curves TG and DTA. The measurements were performed at the temperature range from 30 to 1100 °C with a heating rate 10 $°C \cdot min^{-1}$ with a sample weight approx. 60 mg in corundum crucibles and air atmosphere.

RESULTS AND DISCUSSION

By the XRD analysis, two distinct structures of hydroxyapatite have been identified: monoclinic and hexagonal. Figure 1 shows the diffractogram of sample 1 containing the hydroxyapatite diffraction line $Ca_{10}(PO_4)_6(OH)_2$ with the parameters: hexagonal crystalline system; space group $P6_3/m$. Figure 1 also demonstrates a diffractogram of sample 2 containing the hydroxyapatite diffraction line $Ca_{10}(PO_4)_6(OH)_2$ with the parameters: monoclinic crystalline system; space group $P2_1/b$. For samples 3 and 4, diffraction lines with the following parameters were identified: hexagonal crystalline system; space group $P6_3/m$. The XRD profiles of both structures are almost identical, it means that both crystalline structures are very similar. For this reason, it is very difficult to properly recognize these structures from the XRD profiles of the measured samples. These structural types of hydroxyapatite were selected based on the lowest value of FOM (figure of merit), i.e. based on the best match.

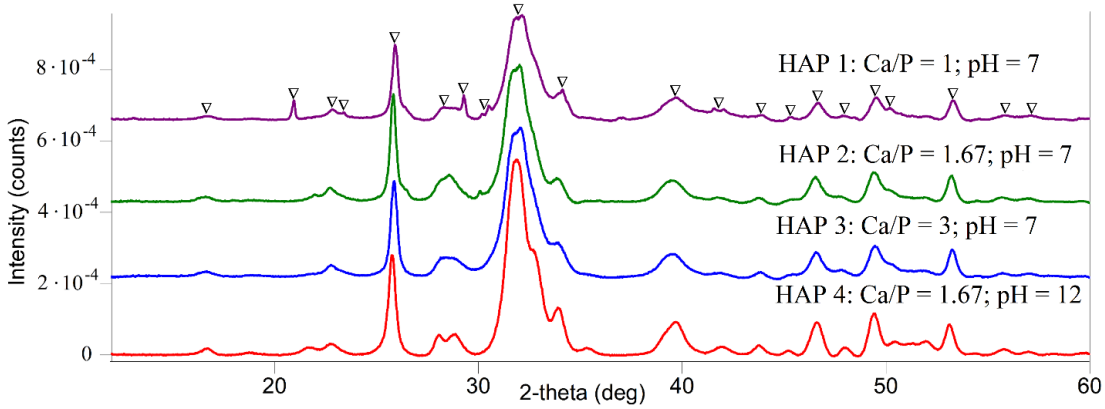

Fig. 1 *Diffractogram of crystal system of hydroxyapatite.*

Core lines of elements and binding energy of hydroxyapatite were detected by the XPS analysis. The XPS image performances the XPS spectrum for sample HAP 1 (Ca/P = 1, pH = 7). The core lines of the elements (Ca 2p, O 1s, P 2p) and Auger electrons of the hydroxyapatite are shown in Figure 2. Auger electrons have binding energy for Calcium LMM 1196.55 ± 0.3 eV and Oxygen KLL 978.05 ± 0.3 eV (Table 2).

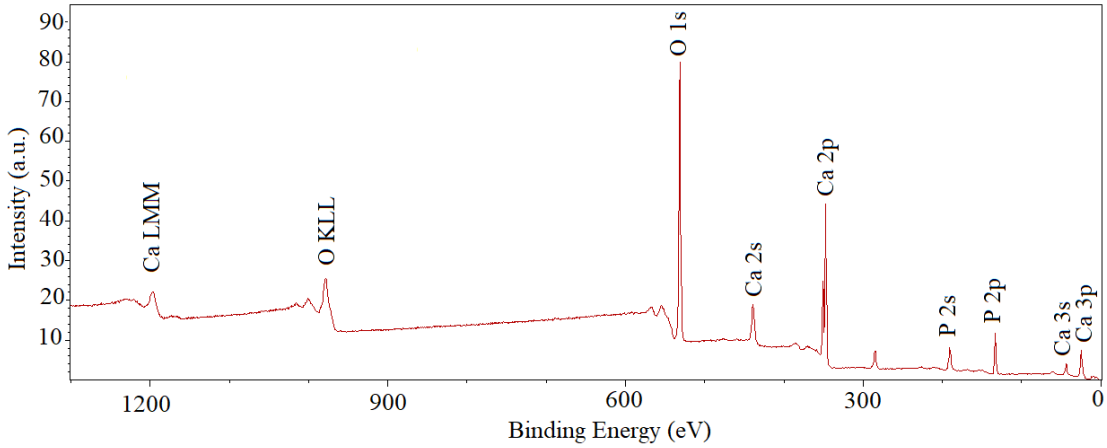

Fig. 2 *The core lines and binding energy of hydroxyapatite.*

Tab. 2 *Binding energy and core levels of hydroxyapatite.*

Element	Core levels	Binfing energy (eV)
Calcium	LMM	1196.55 ± 0.3
Oxygen	KLL	978.05 ± 0.3
Oxygen	1s	531.03 ± 0.3
Calcium	2s	440.20 ± 0.3
Calcium	2p	347.04 ± 0.3
Phosphor	2s	190.20 ± 0.3
Phosphor	2p	133.03 ± 0.3
Calcium	3s	45.40 ± 0.3
Calcium	3p	26.40 ± 0.3

According to DTA/TG analysis, the impact of the Ca/P ratio was proven (Figure 3 and 4, Table 2). There is conformity that the thermal behavior of HAP occurs in a four-stage process including dehydroxylation and decomposition [14]:

- Stage 1: $Ca_{10}(PO_4)_6(OH)_2 \rightarrow Ca_{10}(PO_4)_6(OH)_{2-2x}O_x\square_x + x\ H_2O$
  (hydroxyapatite) (oxyhydroxyapatite)

- Stage 2: $Ca_{10}(PO_4)_6(OH)_{2-2x}O_x\square_x \rightarrow Ca_{10}(PO_4)_6O + (1\text{-}x)\ H_2O$
  (oxyhydroxyapatite) (oxyapatite)
- Stage 3: $Ca_{10}(PO_4)_6O \rightarrow 2\ Ca_3(PO_4)_2 + Ca_4(PO_4)_2O$
  (oxyapatite) (tricalcium phosphate) (tetracalcium phosphate)
- Stage 4: $Ca_4(PO_4)_2O \rightarrow 4\ CaO + P_2O_5\uparrow$ or $Ca_3(PO_4)_2 \rightarrow 3\ CaO + P_2O_5\uparrow$

The first stage, dehydroxylation, incorporates the loss of water, which proceeds through the formation of oxyhydroxyapatite (OHAP) and then oxyapatite (OHA; second stage) where □ stands for a lattice vacancy in the OH position along the crystallographic c-axis. Decomposition of OHA then proceeds to secondary phases such as tricalcium phosphate (β–TCP) and tetracalcium phosphate (T–TCP; third stage). The transformation of HAP has important consequences in bone engineering and plasma coated implants, since β–TCP is resorbable calcium phosphate, and while it will enhance resorption of HAP implants, decomposition of HAP will also reduce the mechanical properties of the material.

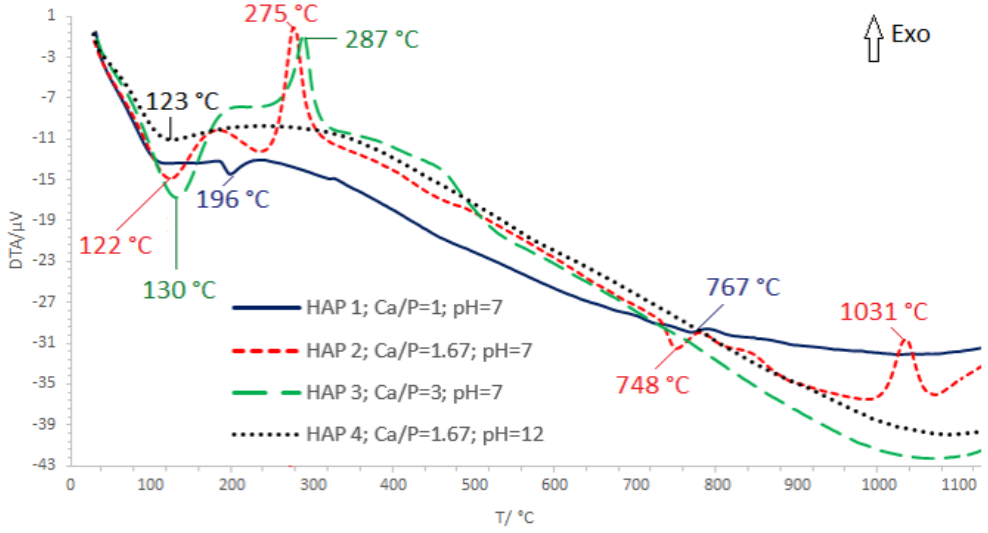

Fig. 3 *DTA curves of HAP samples prepared for different Ca/P ratios and pH.*

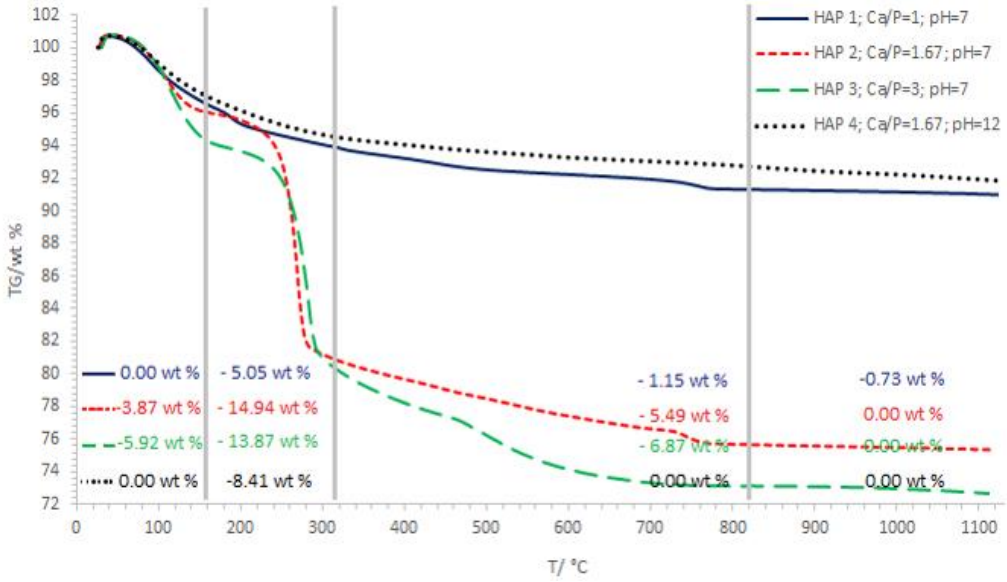

Fig. 4 *TG curves of HAP samples prepared for different Ca/P ratios and pH.*

Tab. 3 *Overview of processes occurring during hydroxyapatite decomposition.*

Sample	TA results					Process
	T_{range} (°C)	Δm (%)	TA effect	T_{peak} (°C)	Total Δm (%)	
1	80–350	5.05	endo	196	9.15	dehydration
	600–900	1.15	endo	767		dehydroxylation→ →OHAP→OHA; OHA→β–TCP and T–TCP
2	70–180	3.87	endo	122	24.81	dehydration
	180–500	14.94	exo	275		elimination of ammonia
	550–800	5.49	endo	748		dehydroxylation→OHAP→ →OHA; OHA→β–TCP and T–TCP
	900–1050	–	exo	1031		decomposition of T–TCP in CaO and $Ca_3(PO_4)_2$
3	80–180	5.92	endo	130	27.65	dehydration
	180–330	13.87	exo	287		elimination of ammonia
	350–800	6.87	–	–		unidentified
4	100–220	–	endo	123	8.41	dehydration

Table 3 provides a summary of the processes that occur during hydroxyapatite decomposing. With the decomposition of sample 1 (precipitation parameters: a ratio of Ca/P = 1; pH = 7), the dehydration of the sample first occurs (196 °C). Subsequently, dehydroxylation occurs to form oxyhydroxyapatite (OHAP), which is transformed into oxyapatite (OHA) which decomposes to form β–TCP and T–TCP (767 °C). With the decomposition of sample 2, which was synthesized at the ratio of Ca/P = 1.67 and pH = 7, the dehydration of the sample first occurs (122 °C). Then ammonia is eliminated (275 °C). Subsequently, dehydroxylation occurs to form OHAP, which is transformed into OHA (748 °C). Then the decomposition of oxyapatite follows, which decomposes to form β–TCP and T–TCP (748 °C). T–TCP is then spread into CaO and $Ca_3(PO_4)_2$ (1031 °C). With the disintegration of sample 3 (synthesis parameters: the ratio of Ca/P = 3; pH = 7), the dehydration of the sample first occurs (130 °C). Subsequently, ammonia is eliminated (287 °C). The last endothermic peak, in the temperature range of 350–800 °C, was not identified. With the decay of sample 4, which was prepared at the ratio of Ca/P = 1.67 and pH = 12, the dehydration of the sample occurs (123 °C). No more peaks in the temperature range of 220–1000 °C were identified.

CONCLUSION

The synthesis conditions (Ca/P ratio = 1, 1.67, 3 and pH = 7, 12) are suitable for the formation of crystalline hydroxyapatite. From the results of XRD analysis is clear, that two distinct structures of hydroxyapatite have been identified: monoclinic and hexagonal. The XPS spectrum involves the core lines of the elements (Ca 2p, O 1s, P 2p) and Auger electrons of the hydroxyapatite. Auger electrons have binding energy for Calcium LMM 1196.55 ± 0.3 eV and Oxygen KLL 978.05 ± 0.3 eV. By DTA/TG analysis, the effect of the Ca/P ratio was proven. Thermal behavior of HAP occurs in a four-stage. Decomposition of OHA proceeds to secondary phases such as β–TCP and T–TCP.

Generally, the best results were obtained in sample 1, which was synthesized at a ratio of Ca/P = 1, the value of pH = 7 and a precipitation rate of 2 ml/min. This claim is based on all the analyzes executed, especially with regard to crystallinity (the smallest crystallite size), shape and size of particles (thin needles and tabular plates), particle size distribution (the

narrowest range of particle size), hexagonal crystalline system (space group P63/m) and thermal behavior (produced products β–TCP and T–TCP). By contrast, less suitable precipitation conditions at the Ca/P ratio = 3 were demonstrated (sample 3; bulky formation; the widest range of particle size), and from a thermal behavior aspect, less favorable results at the value of pH = 12 were proved (sample 4, non-expressive peaks). From the gained results we can confirm that the Ca/P ratio and the value of pH have an effect on the particle morphology as well as its thermal behavior.

Authors would like to thank for financial support to Internal Grant Agency of the University of Pardubice (SGS_2019_004).

REFERENCES

[1] Elliott J.C.: Structure and chemistry of the apatites and other calcium orthophosphates, Elsevier (1994).
[2] Rivera-Muñoz E.M.: Hydroxyapatite - based materials: synthesis and characterization, Intech (2011).
[3] Friedman H.: The apatite mineral group (2014).
[4] Kalendová A.: Technologie nátěrových hmot I, Univerzita Pardubice (2003).
[5] Yang Y.H, Liu C.H, Liang Y.H, Lin F.H, Wu K.C.W.: J Mater Chem. 1 (2013) 2447.
[6] Jarcho M, Bolen C.H, Thomas M.B, Bobick J, Kay J.F, Doremus R.H.: J Mater Sci. 11 (1976) 2027.
[7] Meejoo S, Maneeprakorn W, Winotai P.: Thermochim Acta. 447 (2006) 115.
[8] Kumta P.N, Sfeir C, Lee D.H, Olton D, Choi D.: Acta Biomater. 1 (2005) 65.
[9] Wang P.E, Chaki T.K.: J Mater Sci-Mater M. 4 (1993) 150.
[10] Tampieri A, Celotti G, Szontagh F, Landi E.: J Mater Sci-Mater M. 17 (1997) 1079.
[11] Savino K, Yates M.Z.: Ceram Int. 41 (2015) 8568.
[12] Sun R, Chen K, Liao Z, Meng N.: Mater Res Bull. 48 (2013) 1143.
[13] Hermassi M, Valderrama C, Dosta J, Cortina J.L, Batis N.H.: Chem Eng J. 267 (2015) 142.
[14] Chetty A.S, Wepener I, Marei M.K, Kamary Y.E.L, Moussa R.M.: Synthesis, properties, and applications of hydroxyapatite, New York (2012).